Byzantine wall paintings from San Marco d'Alunzio, Sicily: non-invasive diagnostics and microanalytical investigation of pigments and plasters

Maria Francesca Alberghina[1,2], Maria Antonietta Zicarelli[1], Luciana Randazzo[3*], Salvatore Schiavone[2], Mauro Francesco La Russa[1], Maria Labriola[4], Davide Rigaglia[4] and Michela Ricca[1*]

Abstract

A diagnostic investigation was carried out on twelfth century Byzantine wall paintings preserved in the Museum of Byzantine and Norman Culture and Figurative Arts of San Marco d'Alunzio (Messina, Italy) on the occasion of recent restoration works. First, the wall paintings were analyzed using portable X-Ray Fluorescence (p-XRF) and Fiber Optics Reflectance Spectroscopy (FORS) to obtain a non-invasive preliminary identification of the original palette. Then, five fragments were sampled for a micro-stratigraphy study using Digital Optical Microscope (DOM), Polarizing Optical Microscope (POM), and Scanning Electron Microscopy (SEM) combined with Energy Dispersive X-ray Spectrometry (EDS) to characterize the mortars and the blue and black pigments non unequivocally identified through non-invasive techniques. The palette included mainly earthen pigments like red and yellow ochres, green earth, and more valuable lapis lazuli blue applied on a bone black layer; while the analysis of mortars found on the different apses showed the same manufacturing technique and constitutive materials: lime-based binder with the addition of quartz, and rare calcareous lithic fragments as aggregate. The obtained results shed light on the pictorial technique used for the wall paintings and allowed us to compare the Sicilian pictorial cycle with the coeval Byzantine wall paintings preserved in Sardinia and Southern Italy.

Keywords Byzantine wall paintings, Pigment, Plaster, Lapis lazuli, p-XRF, FORS, SEM–EDS, POM

Introduction and description of the wall paintings

The subject of this study are two apsidal wall paintings currently preserved inside the Museum of Byzantine and Norman Culture and Figurative Arts of San Marco d'Alunzio, in the province of Messina (Sicily) (Fig. 1A–D).

Established in 1997, the museum incorporates the remains of a church from the Byzantine-Norman period, accidentally discovered in 1953 by the scholar Domenico Ryolo [1, 2]. Following the discovery, the building was referred to as the 'Church of the Holy Savior' or the 'Church of the Four Holy Doctors,' in reference to the subject of the paintings preserved within the structure [1].

*Correspondence:
Luciana Randazzo
luciana.randazzo@unipa.it
Michela Ricca
michela.ricca@unical.it
[1] Department of Biology, Ecology and Earth Sciences (DiBEST), University of Calabria, 87036 Arcavacata di Rende, CS, Italy
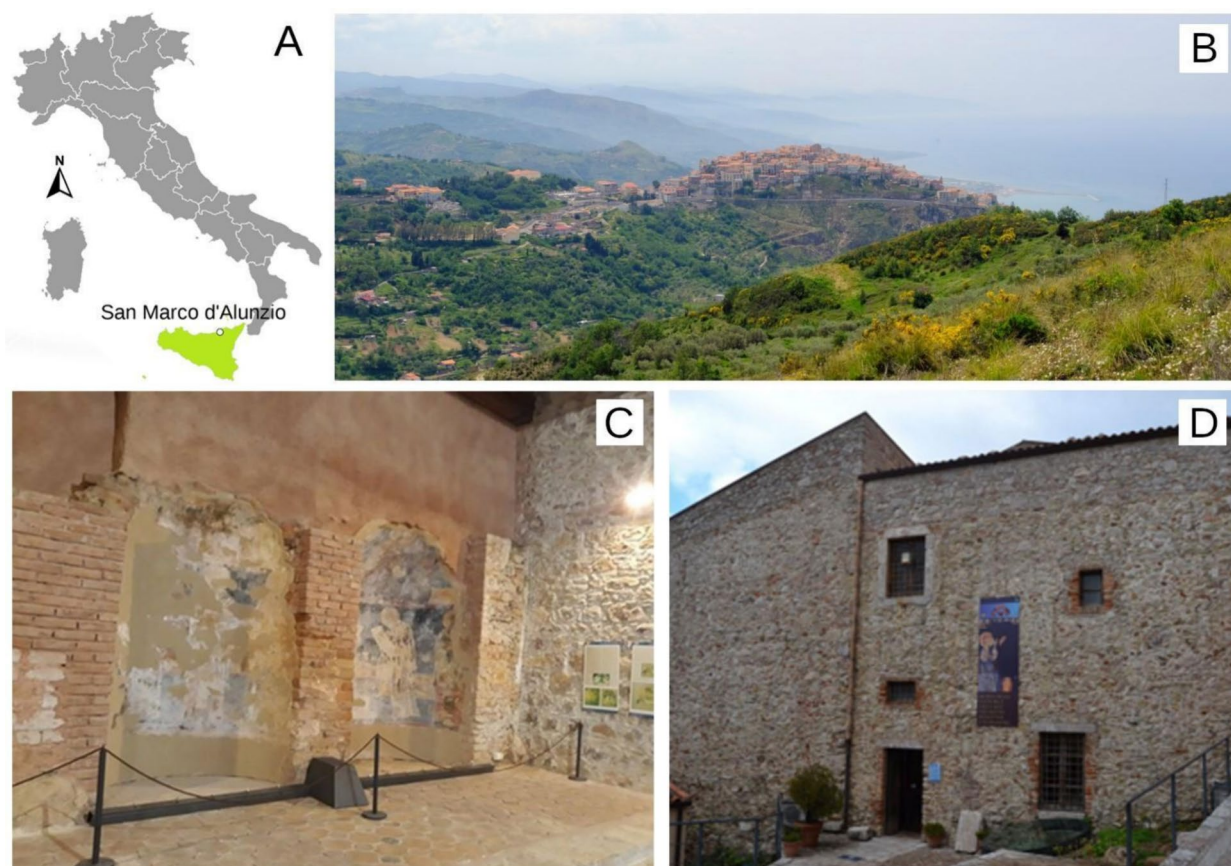[2] S.T.Art-Test, Via Stovigliai, 88, 93015 Niscemi, CL, Italy
[3] Department of Earth and Marine Sciences (DiSTeM), University of Palermo, 90123 Palermo, PA, Italy
[4] Consorzio PRAGMA – Restauro e Conservazione dei Beni Culturali, via della Pisana 247, 00163 Rome, Italy

Alberghina *et al. Heritage Science*   (2024) 12:184

Page 2 of 17

Fig. 1 Location of San Marco d'Alunzio in the Sicily region (**A**); View from the top of San Marco d'Alunzio (Image reproduced under Creative Commons—Attribution-ShareAlike 4.0 International license—Davide Mauro author (https://it.m.wikipedia.org/wiki/File:Panorama_di_San_Marco_d%27Alunzio.jpg), "Panorama di San Marco d'Alunzio") (**B**); Museum of Byzantine and Norman Culture and Figurative Arts in San Marco d'Alunzio (**C**); The two apsidal wall paintings before the restoration work of 2020 (**D**)

The two apse basins were the first architectural elements to be uncovered. Subsequently, once the structure was cleared of earth and rubble, the ancient architectural configuration of the building came to light.

The church appeared to be a singular rectangular space, oriented to the east and characterized by a single entrance located along the western side. The eastern wall, leaning against a rocky slope, housed three apses: the *prothesis (in cornu epistolae* apse), the central apse, and the *diaconicon* (*in cornu evangelii* apse). While the central apse and the *prothesis* are still observable, unfortunately, the *diaconicon* was destroyed before the discovery [1].

The two surviving apses preserve valuable pictorial evidence in a distinctly Byzantine style, unfolding within an elaborate iconographic program. The dating of the wall paintings has long been the subject of debate among historians. Early studies conducted by Ryolo assigned the paintings to the pre-Norman period and more accurately in the second half of the twelfth century [1], while

Edward Kislinger attributed them more broadly to the eleventh century [3]. However, according to the most recently proposed hypothesis, the paintings could be dated from the twelfth century to the first decades of the thirteenth century [4–6].

The fragmentary state of preservation of the paintings in the central apse hinders the complete understanding of the entire composition. (Fig. 2A). The dominant figure in the conch area is Christ *Pantocrator*, of which only a portion of the chest and the left are preserved. Due to the compositional structure and the peculiar decoration of the garment, the Christ of San Marco d'Alunzio appears to be similar to the one preserved inside the Cathedral of Monreale (Palermo, Sicily) [2]. Below the semi-dome, four standing figures with halos are barely recognizable and generally identifiable as holy bishops.

The decoration in the right apse is the best preserved and represents the Virgin with the Child in the conch and the four Doctors of the Eastern Church in the semi-cylindrical area (Fig. 2B). In the center of the semi-dome,

Fig. 2 The central (**A**) and the right (**B**) apsidal wall paintings after the restoration work of 2020

the Virgin is depicted according to the iconography of the *Glykophilousa* holding the Child in the act of taking steps. The angel to the left, facing the Virgin, holds a censer, while the one to the left, at first documented by Ryolo, has been irremediably lost.

The representation in the conch, both for the naturalistic execution of the angel's face and for the depicted theme, reveals elements of absolute innovation in the contemporary Sicilian artistic panorama. Even if the iconography of the representation of the Virgin within the semi-dome is attested in the same period in other examples from Campania, the *Glykophilousa* in the 'Church of the Four Holy Doctors' represents an *unicum* in the Sicilian region both for its iconography and the privileged position in the apse [2].

In the semicylindrical area below the apse conch, the four Doctors of the Eastern Church are depicted standing at the sides of an altar on which rest a chalice and a paten. The identification of the saints relies not only on their physiognomic features but also on the Greek inscriptions depicted next to them in the background. Saint Basil and

Saint John Chrysostom appear centrally in the scene, facing an altar and holding an unfurled scroll where it is possible to read excerpts from the *Anaphora* of Saint Basil. Both are represented with halos and heads inclined as a sign of reverence towards the altar, adorned in rich garments, and with bearded and emaciated faces, in line with the canons of Byzantine art. The other two figures, in a frontal position and painted on the lateral sides of Saint Basil and Saint Chrysostom, are respectively Saint Athanasius on the left, and Saint Gregory of Nazianzus on the right.

It seems quite evident that the moment of the liturgy plays a primary role in the iconographic theme depicted. This is rather unusual evidence for other contemporary mural paintings in southern Italy, in which the liturgical role did not seem to affect the elaboration of the iconographic programs. Nevertheless, stylistic and iconographic similarities can be traced with some Byzantine pictorial testimonies from Apulia, Lucania, and Calabria (Southern Italy): in particular with the paintings of Santa Maria delle Cerrate in Squinzano (Lecce), those of Santa

Alberghina *et al. Heritage Science*   (2024) 12:184

Page 4 of 17

Maria in Anglona (Matera), the pictorial decoration in the Cattolica di Stilo (Reggio Calabria), and the paintings of the Panaghia in Rossano (Cosenza). However, judging from the execution of the robes and faces of the saints, from the novel elements and the technique used, the example of San Marco d'Alunzio seems marked by a greater stylistic maturity, bringing it closer to the thirteenth century [2].

Conservation history and restoration works

The conservation history of the pictorial evidence present in the Church of the Four Holy Doctors is marked by a series of events that have significantly compromised their state of conservation starting from the time of built. At the time of discovery, the paintings appeared obliterated by a layer of masonry and only a few traces of painted plaster could be recognized beneath it [1]. Due to the long period that passed from the discovery to the beginning of the conservation and protection work of the paintings, several collapses occurred which affected part of the semi-domes, resulting in a substantial loss of the pictorial decoration. This is clearly demonstrated by the fact that the brick arches and the right angel in the *prothesis*, previously described by the sources, are no longer visible today. Once the work began and the layer of masonry was removed from the apse area, a past attempt to hide the wall paintings in ancient times became evident, as a thin layer of lime covered them [1].

Then, once the paintings were discovered and efforts continued to free the church structures from the ground, a fence, and a roofing system were built to prevent vandalism and protect the pictorial testimonies from atmospheric agents.

The worsening of the conservation conditions of the pictorial evidence is probably attributable not only to the neglect following the discovery but also to the variation of the thermo-hygrometric equilibrium that occurred due to the excavation [2]. In fact, the unearthing of the walls would have favored the rapid evaporation of humidity with the consequent crystallization of the soluble salts within the structure leading to the formation of lacunae and causing the loss of the pictorial film.

Only at the end of the 1990s, on the occasion of the museum construction, the paintings underwent the first restoration work.

Due to a lack of documentation, it is only possible to hypothesize what procedures and materials were adopted. Essentially, it can be stated that the restoration intervention concerned an in-depth consolidation, aiming to address adhesion defects between the plaster and the support, along with a cleaning, thus restoring greater readability of the artwork. However, to secure both the plaster and the mortar and to fill the existing lacunae, the products used, such as cement mortars, epoxy resins, and gypsum, were incompatible with the original materials. Overall, the reintegration intervention seems to have been carried out without a unified methodology, and produced the opposite effect to the expected, making it more difficult to read the entire composition [2].

In 2020, 30 years after the first restoration intervention, a new conservation work was planned. Following the principles of minimal intervention, the operations initially involved the stabilization of the plaster fragments and restoring of the adhesion between the preparatory layers and the support. Then, both physical and chemical methods were used to remove salt efflorescences and inadequate stucco plastering, allowing the recovery of valuable portions of the paint film and the original mortar, hidden under the plaster of the previous intervention. Specifically, before removing the plaster, the painted areas were secured by covering them with Japanese paper using 20% Paraloid B72 dissolved in acetone. Subsequently, a poultice was applied by soaking cotton in acetone, facilitating the removal of the gypsum layer mixed with acrylic polymers. The final phase involved the *a tono* reintegration of the continuity solutions in correspondence with the small *lacunae* and abrasions of the pictorial film, and the reintegration of the *lacunae* of the pictorial film through the "*rigatino*" method, on the background and the architectural elements [2]. Instead, in correspondence with small lacunae in the figurative subjects, which involve the different depths along the stratigraphy and in some cases up to the wall structure due to the loss of *arriccio* and *intonachino* layers, the conservative intervention involved the remake of only the *arriccio* by means of sub-level plastering, with a mortar in terms of grain size and color very similar to the original, guaranteeing continuity of behavior and protection to the original surfaces.

Finally, for the large *lacunae* affecting the superficial level of pictorial application of the apses, pictorial additions were not carried out but the tone of the plaster was uniformed to highlight and facilitate the reading of small and medium isolated traces of pictorial surface still preserved.

This conservative intervention favored the correct reading of the paintings, providing information on the executive techniques used by the artists. The executive works were accompanied at all stages by an extensive diagnostic survey, which allowed the identification of the raw materials and the comparison of the two paintings under investigation. The investigation was initially carried out using portable and non-invasive instrumentation (i.e., XRF and FORS), preliminarily characterizing the pigments used. Then, to overcome the limitations sometimes emerging from the use of portable

Alberghina *et al. Heritage Science*   (2024) 12:184

Page 5 of 17

instrumentation in situ, more in-depth studies were carried out with microscopic techniques (i.e., DOM, POM, SEM–EDS) following the collection of micro-samples. Achieved results were fundamental to characterizing the pigments and providing detailed information on both the stratigraphy and the raw materials used in the past in wall painting.

Sampling and analytical methods

Wall paintings were investigated using both in situ and laboratory investigations. Details about in situ measurements, micro-fragments sampling, and the analytical techniques employed are described in Tables 1 and 2.

At first, an in situ and non-invasive investigation was conducted for the preliminary identification of both areas of study (i.e., the two apsidal wall paintings) and pigments.

The first approach to the pictorial evidence consisted of a careful macroscopic observation conducted through visual examination followed by an investigation of the painted surfaces with the Digital Optical Microscope (DOM). The DOM used is a DINOLITE AM4113T-FVW (Dino-Lite Europe, IDCP B.V. 1321 NN Almere The Netherlands), performed in visible light and ultraviolet (UV) light at 50 and 200 magnifications with the following technical characteristics: Resolution: 1.3 Mpixels, Magnification: $10\times \div 50\times$; $200\times$, Illumination: 4 UV LEDs with 400 nm + emission; 4 built-in white LEDs, Sensor: Color CMOS, Manual calibration and Measurement with accuracy around ± 3 μm. The instrument

Table 1 Description of the in-situ investigations carried out on the wall painting in the right apse

| Measurement point ID	Performed analyses	Measurement area	Color
P1	p-XRF	Saint John Chrysostom's robe	Red pictorial layer
P2	p-XRF	Saint John Chrysostom's pallium	Light-yellow pictorial layer
P3	p-XRF	Background decorative band	Dark-yellow pictorial layer
P4	p-XRF	Saint John Chrysostom's pallium	Green pictorial layer
P5	p-XRF	Chalice's foot	Blue pictorial layer
P6	p-XRF	Saint John Chrysostom's beard	Brown pictorial layer
P7	p-XRF	Saint John Chrysostom's eye	Dark-green pictorial layer
P8	p-XRF	Greek inscription in the background	White pictorial layer
P9	p-XRF	Background	Black pictorial layer
P10	FORS	Saint Athanasius' robe	Dark-red pictorial layer
P11	FORS	Saint Athanasius' robe	Light-red pictorial layer
P12	FORS	Saint Athanasius' eye	Dark-green pictorial layer
P13	FORS	Saint John Chrysostom's eye	Dark-green pictorial layer
P14	FORS	Saint John Chrysostom's pallium	Light-green pictorial layer
P15	FORS	Saint John Chrysostom's robe	Blue pictorial layer
P16	FORS	Chalice's node	Blue pictorial layer
P17	FORS	Chalice's cub	White pictorial layer
P18	FORS	Saint John Chrysostom's face	Brown pictorial layer
P19	FORS	Background	Dark-yellow pictorial layer
P20	FORS	Saint John Chrysostom's pallium	Light-yellow pictorial layer

Table 2 List of the micro-samples taken from the wall painting surfaces

Sample ID	Description	Sampling location	Employed analyses
SM1	Fragment including both plaster layers and the greyish-bluish pictorial film	Background, central apsidal wall painting	DOM, XRF
SM2	Sample representative of the painting stratigraphy	Central apsidal wall painting	POM, DOM
SM3b	Fragment including both plaster layers and the greyish-bluish pictorial film	Background, central apsidal wall painting	DOM, XRF
SM4	Fragment including both plaster and the blue and black pictorial film	Background, semi-dome area, right apsidal wall painting	DOM, SEM–EDS
SM5	Sample representative of the painting stratigraphy	Right apsidal wall painting	POM, DOM

Alberghina *et al. Heritage Science*   (2024) 12:184

Page 6 of 17

allowed us to select idoneous measurement points and areas, avoiding areas of retouching or remaking. Following that, a portable X-Ray fluorescence spectroscopy (p-XRF) was employed on nine sample points (Table 1, Fig. 3) to determine, at the elemental scale, the composition of the most representative painted areas, in terms of major and minor constituents [7, 8].

In particular, XRF analysis was carried out on the pictorial surfaces in correspondence of the right apse with the representation of the four Doctors of the Eastern church (Fig. 3). The good state of conservation of the painted layers and their representativeness for characterizing the whole color palette drove the choice to carry out the non-invasive measurements only on the right apse. XRF spectra were collected through a XRF spectrometer by AMPTEK (Bedford, MA 01730, USA). It consists of a miniature X-ray tube system Mini-X—Amptek, which includes the X-ray tube (max voltage of 40 kV, max current of 0.2 mA, target Rh, collimator 1 or 2 mm), the power supply, the control electronics and the USB communication for remote control; a Silicon Drift Detector (X-123SDD—Amptek) with a 125–140 eV FWHM @ 5.9 keV Mn Kα line Energy Resolution (depends on peaking time and temperature); 1–40 keV Detection range

of energy; max rate of counts to 5.6×10^5 cps; software for acquiring and processing the XRF spectra. Primary beam and detector axis form an angle of 0 and 40 degrees respectively with the perpendicular to the sample surface. Measurement parameters were as follows: tube voltage 35 kV; current 80 μA, acquisition time 60 s; no filter was applied between the X-Ray tube and the sample; distance between sample and detector around 1 cm. The setup parameters were selected to have a good spectral signal and to optimize the signal to noise ratio (SNR). The color palette of the artists was then analyzed using Fiber Optics Reflectance Spectroscopy (FORS) to obtain further data confirming the identification of the chromophores already detected by the previous investigation. Measurements were performed in the visible-near infrared spectral range (400÷950 nm) by using a tungsten lamp (BeWTek, Inc. BPS101 Tungsten Halogen Light Source with a spectral output of 350–2600 nm) as source and the grating AFBR-S20M2WV Qmini Broadcom (Palo Alto CA) equipped with optical fibers as detector as detector. The measuring head allows to collect the reflected radiation at 45° in an analyzed area of about 2 mm². Each acquired spectrum was the average of 64 scans. As a reference, a 99% reflective Spectralon® plate was used. The
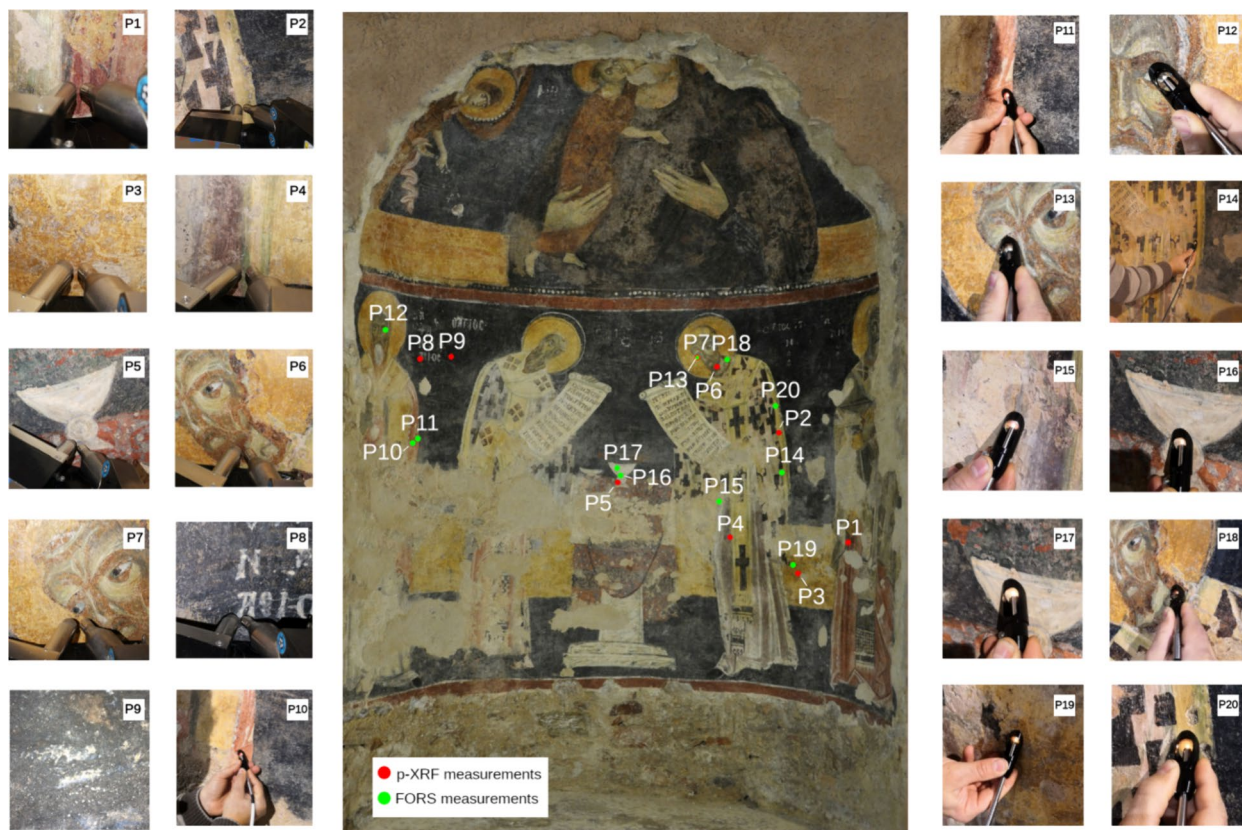
Fig. 3 Mapping of the p-XRF and FORS measurement areas performed on the wall painting in the right apse

Alberghina *et al. Heritage Science*　　(2024) 12:184

Page 7 of 17

spectra collected were then compared with those already existing in the literature and with ones available in ISPC-CNR reference database.

Subsequently, five micro-fragments were collected in order to characterize the executive technique and identify the materials constituting the painting stratigraphy (from the *arriccio* to the pictorial layer). Three samples were taken from the central apsidal painting and two fragments were collected from the right one, with the aim to draw comparisons between the two apsidal wall paintings in terms of both constitutive materials and executive technique. A list of the samples, brief description, and analyses performed is shown in Table 2.

In particular, sample SM2, taken from the central apse, and sample SM5, chopped in correspondence with the right apse, were carefully prepared to obtain two thin stratigraphic sections representative of the painting stratigraphy including both the preparatory layers and the pictorial film. Thin sections were then observed under a Polarized Optical Microscope (POM) to examine the minero-petrographic composition, characterize the textural properties, and determine the binder-aggregate ratio. The instrument used was a Zeiss AxioLab microscope (Oberkochen, Germany) equipped with a digital camera to capture images. The microphotographs acquired were afterward compared with those obtained in reflected light using a DOM.

Moreover, a slice of painting (sample SM4) was taken from the black background of the right apse, and a cross-section was prepared. It was preliminarily investigated under visible and UV light by DOM to identify the diverse painting layers.

Subsequently, sample SM4 was analyzed through SEM–EDS to identify the chemical composition of the layers, with particular reference to the few traces of the blue layer juxtaposed with the black one. The aim of SEM–EDS investigation is indeed the identification of the black and blue chromophores, the nature of which could not be unequivocally determined using XRF or FORS due to the intrinsic limits of the two non-invasive methodologies.

Microchemical analyses were obtained employing SEM–EDS ZEISS EVO MA 15 with a W-filament equipped with an analytical energy dispersion system from EDS/SDD, Oxford Ultimax 40 (40 mm^2 with a resolution of 127 eV @ 5.9 keV) and using the Aztec 5.0 SP1 software. The SEM–EDS measurements were performed on carbon-coated cross-sections of the samples with the following operative conditions: an acceleration voltage of 15 kV, 500 pA beam current, working distance between 9 and 8.5 mm.

Again, for comparative purposes, DOM observations and p-XRF analyses were conducted on samples SM1 and

SM3b including the greyish-bluish layer, and collected from the background area of the wall painting in the central apse.

Results and discussion

In-situ measurements

Non-invasive XRF investigations, together with FORS analyses, proved to be particularly effective in shedding preliminary light on the color palette used by medieval artists. The results of both investigations will be presented and discussed below separately by color.

Red and brown pigments

p-XRF spectra acquired in the red-painted areas (P1 measurement point) (Table 1) evidenced peaks of iron, calcium, silicon, sulphur, strontium, and traces of aluminium and barium, indicating the presence of iron oxide compounds such as ochres and/or earth-based pigments and Ca-based compound constituting the underlying plaster, added pictorial layer and do to traces of degradation products still present on surface as visible in corresponding microscope images (Fig. 4A–C) [9–12]. This result is unsurprising since, starting from prehistoric art, ochres, and clay were broadly adopted as pigments thanks to their easy availability in nature and their high stability under different weathering conditions [9, 13, 14]. Their use is also widely attested during the Middle Ages for the execution of mural paintings [15]. The chromophore compound is iron trioxide which is often associated with hydrated aluminum silicates such as kaolinite ($Al_2Si_2O_5(OH)$) and illite (K,H_3O) $(Al)_2(Si,Al)_4O_{10}[(OH)_2,H_2O]$, thus explaining the Si and low Al contribution evidenced in the acquired spectra [16]. Calcium signal was detected in all the investigated areas and might be chiefly ascribed to the underlying lime-based plaster. However, it is important to consider that calcium compounds are generally present in all ochres under the form of calcite ($CaCO_3$), dolomite $[CaMg(CO_3)_2]$, gypsum ($CaSO_4$ $2H_2O$), and/or anhydrite ($CaSO_4$) [16]. The latter assumption could justify the presence of sulphur detected by p-XRF. Sulphur content might also be related to the presence of traces of a "*scialbo*" layer, still visible to the DOM on all the surfaces analyzed. Moreover, while strontium represents a calcium impurity, the trace quantities of barium could be linked to impurities associated with local raw materials or those from near the town [17, 18].

The reflectance spectra collected by FORS in the dark and light red (P10 and P11 measurement points, respectively, Table 1) are characterized by a sharp positive slope between 550 and 600 nm, a maximum around 740–750 nm and an absorption band in the near-infrared region (850–870 nm), therefore confirming the use of a

Alberghina *et al. Heritage Science*   (2024) 12:184

Page 8 of 17
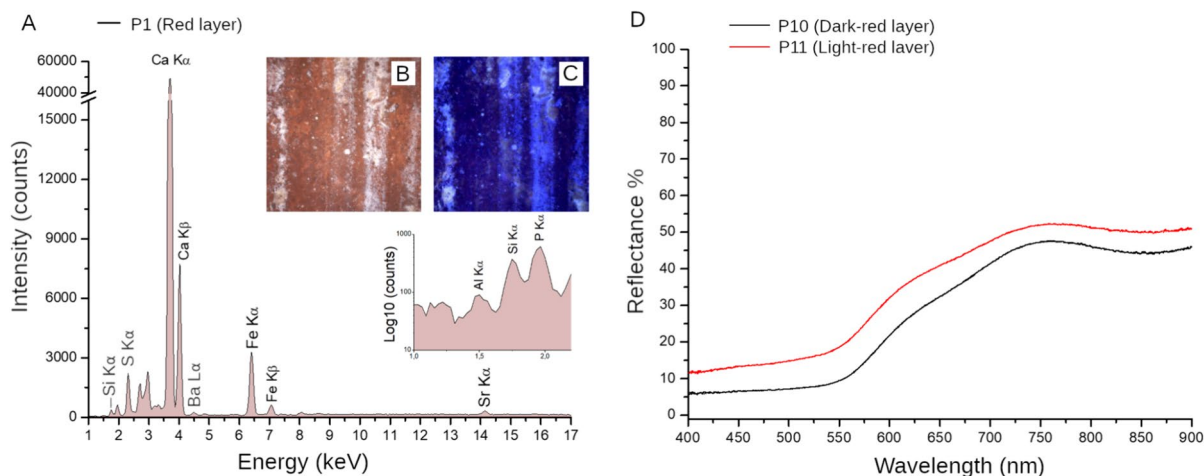
Fig. 4 XRF spectrum acquired in correspondence of the red pictorial layer (P1 measurement point) (**A**); DOM micrographs under visible light (**B**) and UV light (50×magnification) (**C**) of P1 measurement point. FORS spectra of the dark red and light red film (P10 and P11 measurement points) (**D**)

hematite-based pigment (Fig. 4D) [16, 19–22]. The two curves with homothetic trend differ only in reflectance intensity due to the different mixture with lime.

Ochres and/or clay were most likely employed for the execution of the brown-colored areas as well, as evidenced by the presence of calcium, iron, sulphur, potassium, strontium, and traces of silicon identified by the p-XRF (P6 measurement point, Table 1) (Fig. 5A–C). The presence of phosphorus associated with calcium and barium traces (found also in black layer as follow reported) could be interpreted as black bone pigment added in the pictorial mixing to darken the shades of red layers. No Mn signal was detected, thus excluding the

presence of siennas and umbers [23]. Finally, FORS spectra performed on brown areas (P18 measurement point, Table 1) confirmed the presence of hematite as evidenced in Fig. 5D.
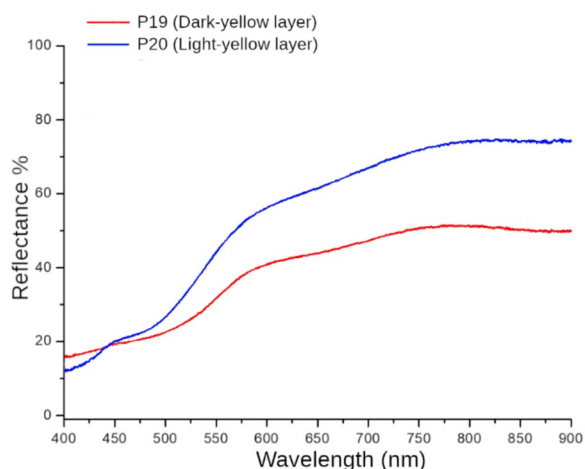
Yellow pigment

The p-XRF spectra detected in the yellowish areas (P2 and P3 measurement points, Table 1) highlight the presence of iron along with the signal of calcium, sulphur, silicon, potassium, and strontium, showing once again, the presence of iron-oxide and clay minerals-based compounds (ochres) [11, 24, 25] (Fig. 6A–E). It is worth considering that, unlike hematite, the
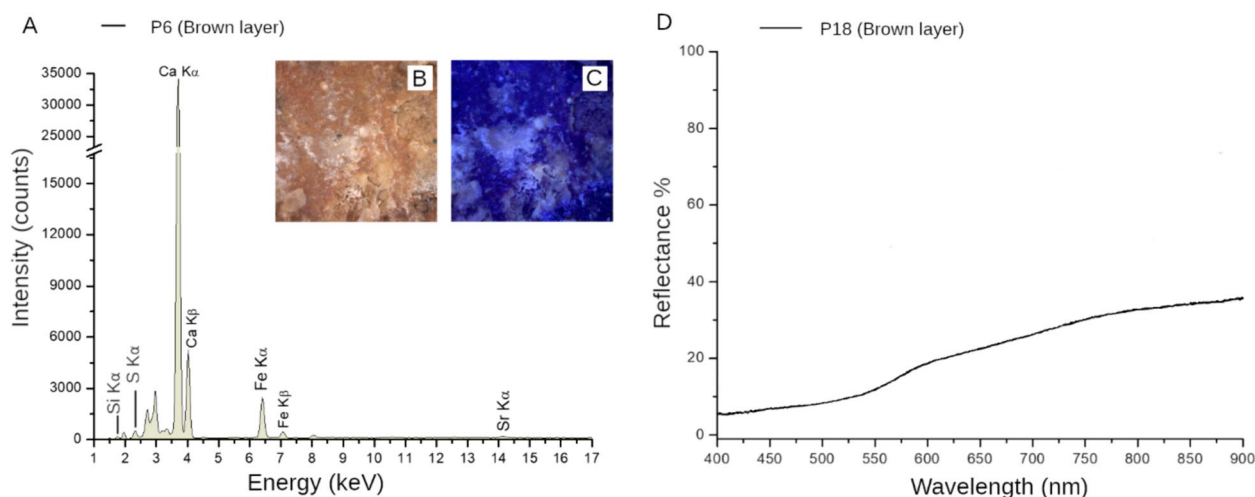
Fig. 5 XRF spectrum acquired in correspondence of the brown pictorial layer (P6 measurement point) (**A**); DOM micrographs under visible light (**B**) and UV light (50×magnification) (**C**) of P6 measurement point. FORS spectrum of the brown film (P18 measurement point) (**D**)

Alberghina *et al. Heritage Science*   (2024) 12:184

Page 9 of 17
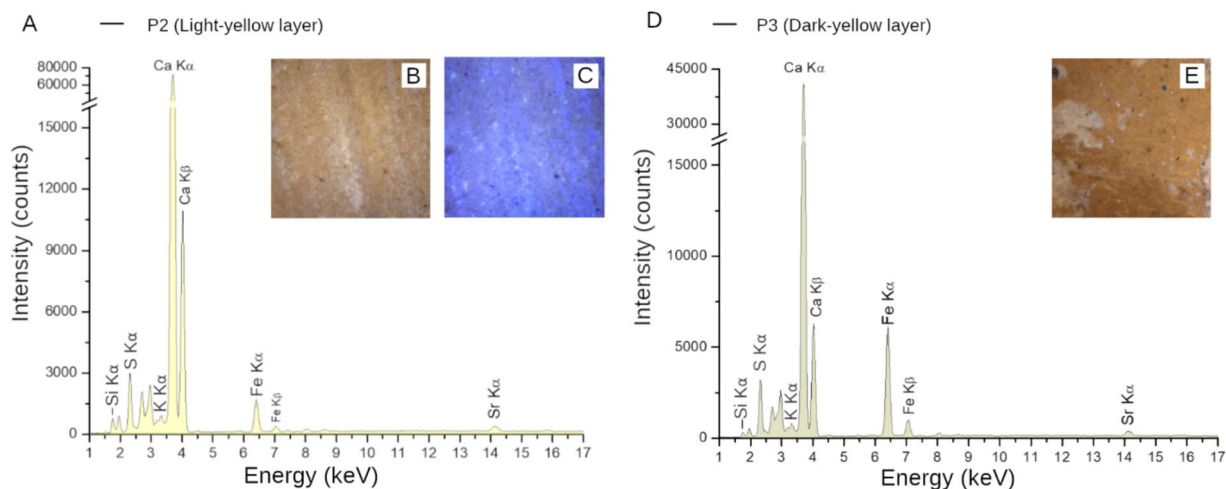
Fig. 6 XRF spectra acquired in correspondence of the light yellow (P2 measurement point) (**A**) and dark yellow (P3 measurement point) (**D**) pictorial layer; DOM micrographs under visible light (**B**, **E**) and UV light (50×magnification) (**C**) of P2 and P3 measurement points

Fig. 7 FORS spectra of the dark yellow and light yellow pictorial films (P19 and P20 measurement points)

chromophore in this case is hydrated iron (III) oxide which gives a typical yellowish hue. The higher calcium counts and slightly lower iron peak in the case of the spectrum acquired at the light-yellow layer might demonstrate the addition of a certain amount of lime to obtain the lighter shades, and determining in the XRF spectra a variable relative intensity between the Ca and Fe characteristic peaks due to the different pictorial matrix.

The reflectance spectra of the yellow areas (P19 and P20 measurement points) (Table 1) show a sharp positive slope starting from lower wavelengths (500–580 nm) with respect to red ochre, and a shoulder in the region between 430 and 480 nm most likely indicating

the use of yellow ochre [22] (Fig. 7). FORS spectra of light-yellow colorations and those of dark-yellow areas reveal overall a similar shape, mainly deferring by their reflectance values (%) once more.

Green pigment

Peaks of calcium, iron, sulphur, potassium, silicon, aluminum, and strontium are again indicative of the presence of iron-oxide-based pigments and clay minerals, suggesting the use of green earth (P4 and P7 measurement points) (Table 1) (Fig. 8A–F). However, the typology of analysis does not allow the discrimination between the use of celadonite and/or glauconite [13, 26, 27]. The p-XRF measurements, carried out on different green areas bearing a darker coloration, show a lower calcium content, absence of potassium and traces of copper probably related to impurities of green pigment, suggesting a different typology of iron-oxide-based pigments mixed or overlapped with calcite, in order to achieve a different greenish hue.

The results obtained from FORS spectra (Fig. 9) acquired on different shades of green pictorial areas (Table 1) indeed exhibit curves typical of green earths, characterized by a maximum of asymmetrical reflection band at around 545÷585 nm, and a broad absorption band centred at 760 nm [19, 20, 28–30].

White and black pigments

The large amounts of calcium together with small contributions of Fe, S, Sr, and Si detected by p-XRF suggest the use of calcium carbonate-based pigment, such as lime white for the white painted areas (P8 measurement point) (Table 1) (Fig. 10A–C) [31].

Alberghina *et al. Heritage Science*   (2024) 12:184

Page 10 of 17
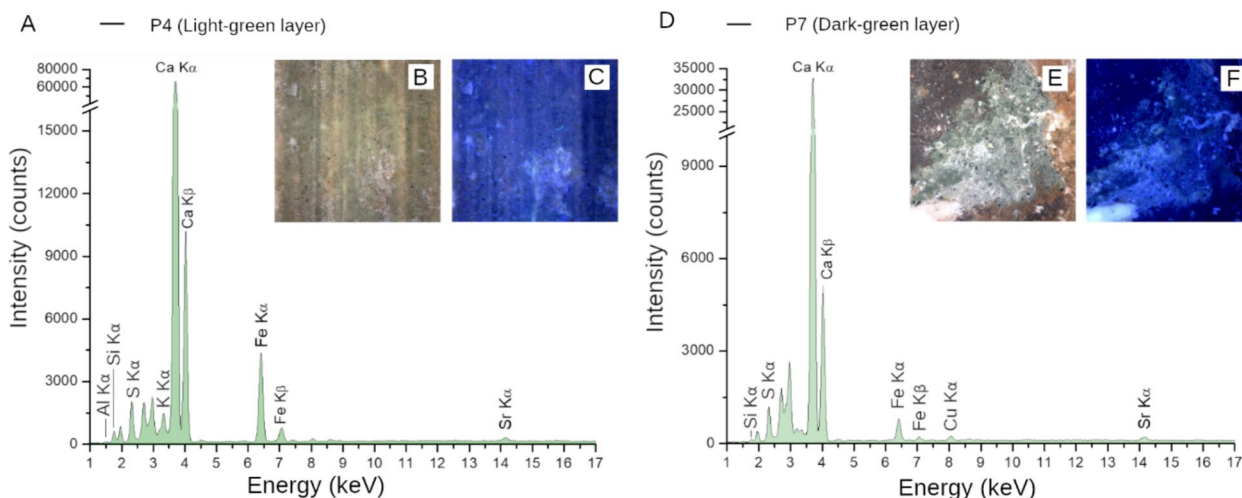
Fig. 8 XRF spectra acquired in correspondence of the light green (P4 measurement point) (**A**) and dark green (P7 measurement point) (**D**) pictorial layer; DOM micrographs under visible light (**B**, **E**) and UV light (50×magnification) (**C**, **F**) of P4 and P7 measurement points
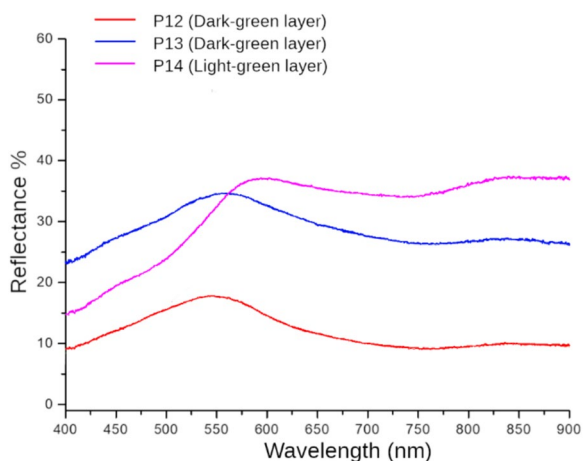
With regard to the black-painted areas, the black chromophore is not detectable by XRF analysis which revealed exclusive peaks of calcium and traces of silicon, iron, and strontium (P9 measurement point) (Table 1) (Fig. 10D–F). The absence of characteristic signals, in fact, suggests the presence of an organic and/or carbonaceous compound. Further in-depth analyses are therefore necessary to fully characterize their nature.

Blue pigment
Based on the XRF data, the blue chromophore used is not clearly identifiable. As a matter of fact, p-XRF spectra of the blue painted areas (P5 measurement point) (Table 1) evidence the presence of calcium, silicon,

sulphur, iron, strontium, potassium, and traces of aluminium (Fig. 11A–C). However, the absence of characteristic peaks referable to other blue pigments historically used, together with the presence of high silicon counts and aluminium and sulphur peaks, allow to hypothesize the use of ultramarine blue [32]. Ca, Fe, and K signals might be attributable in part to impurities deriving from natural lapis lazuli [33]. The low iron counts may otherwise be related to the signal coming from the underlying red-brown layer.

The assumption resulting from the analysis of XRF data was confirmed by FORS investigation. All spectra acquired show in fact the characteristic trend of natural lapis lazuli (Lazurite $(Na, Ca)_8[(S,Cl,SO_4,OH)_2|(Al_6Si_6O_{24})$ with a maximum absorption near 600 nm, a maximum reflectance peak around 500 nm and an inflexion point in the upper region of the visible spectrum (around 675 nm) (P15 and P16 measurement points) (Table 1) (Fig. 11D) [29, 34].

Laboratory-based methods
Characterization of the black and blue pigments and comparison between the two wall paintings
The observations conducted in reflected light using an OM on sample SM4 (Fig. 12A, B) allowed the examination of the painting's stratigraphy, providing additional insights into the executive technique employed for the execution of the wall paintings. The sample, collected from the background of the right apsidal painting and subsequently prepared to obtain a polished cross-section, was examined both in visible and ultraviolet light.

From the acquired micrographs, three distinct layers are clearly distinguishable, from bottom to top:

Fig. 9 FORS spectra of the dark green and light green pictorial film (P12, P13 and P14 measurement points)
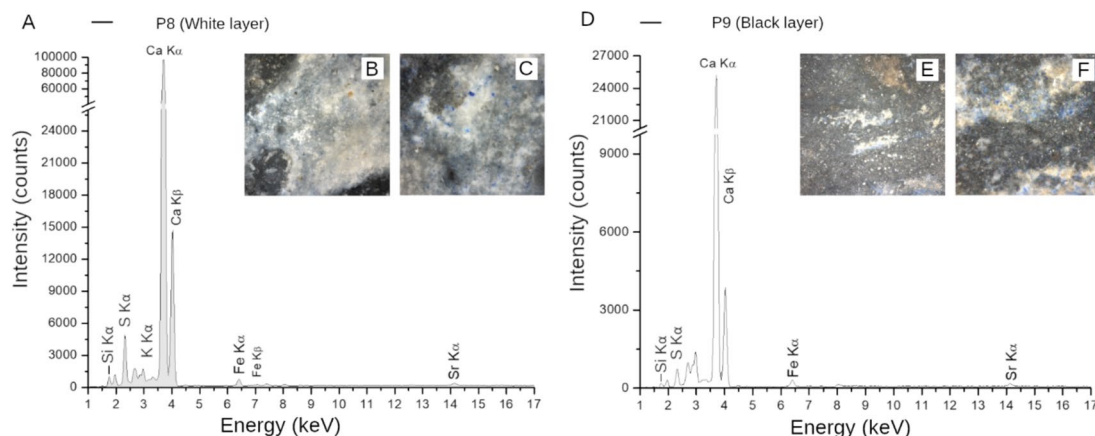
Fig. 10 XRF spectra acquired in correspondence of the white (P8 measurement point) (**A**) and black (P9 measurement point) (**D**) pictorial layer; DOM micrographs under visible light (50×) (**B**, **E**) and 200×magnification (**C**, **F**) of P8 and P9 measurement points
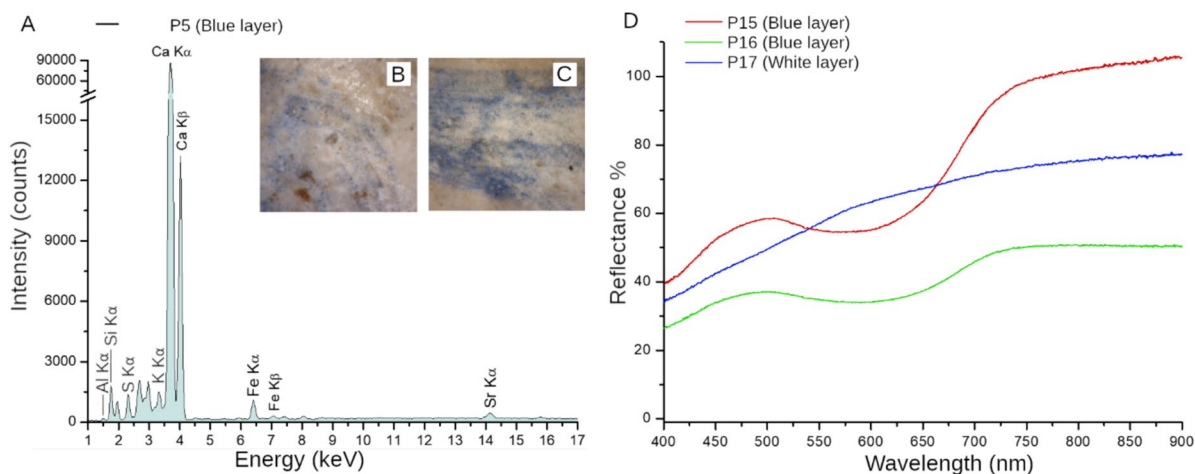

Fig. 11 XRF spectrum acquired in correspondence of the blue pictorial layer (P5 measurement point) (**A**); DOM micrographs under visible light (**B**, **C**) (50X magnification) of P5 measurement point. Reflectance spectra of the blue film (P15, P16, and P17 measurement points) (**D**)

(1) a homogeneous white layer of plaster consisting of a lime-based binder (Fig. 12C, Layer A); (2) a greyish pictorial layer in which numerous small inclusions of black color (ranging in size from a few microns to 30 microns) are identified, dispersed likely within a lime-based binder. The previously described layer has a thickness of approximately 150 µm (Fig. 12C, Layer B); (3) a very thin bluish pictorial layer (approximately 20 µm) containing fine grains of blue color (Fig. 12C, Layer C).

Subsequently, sample SM4 was observed and analyzed using SEM–EDS for the chemical characterization of the raw materials. SEM–EDS results are reported as follows. Layer A is a plaster showing a high lime content. It consists almost exclusively of calcium (92.3%), along with smaller quantities of silicon (3.9%) and other elements (3.8%) (Fig. 13A), as detected by an EDS measurement performed over a large area of the white layer.

The greyish pictorial layer, denominated Layer B, is essentially composed of lime and particles of carbon black of animal origin. Semi-quantitative EDS microanalyses punctually carried out on the black inclusions detected the presence of calcium (67.1%) and phosphorus (31.9%) as well as minor amounts of silicon (0.96%) (Fig. 13B). As shown by the results, calcium and phosphorus are the two primary elements indicative of the presence of the bone black pigment. The latter derives from the carbonizations of bones and it is mainly composed of hydroxyapatite $[Ca_5(OH)(PO_4)_3]$ and coke, produced by the pyrolysis of the collagen inside the bones [15, 35]. In particular, according to Mayer [36], the bone black composition is characterized by 15–20% of carbon, about 20% of calcium sulphate, and around 60% of calcium phosphate.

Alberghina *et al. Heritage Science*   (2024) 12:184

Page 12 of 17
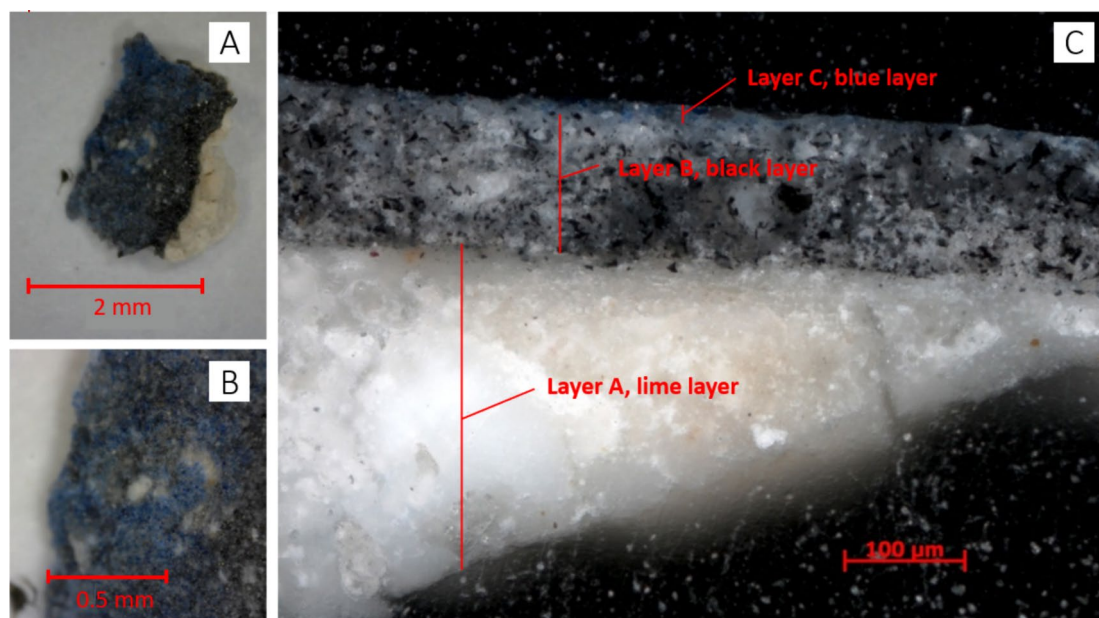
Fig. 12 Micrographs of Sample SM4 before the cross-section preparation (**A**, **B**). Micro-graph of the stratigraphic sample SM4 under reflected light (**C**)
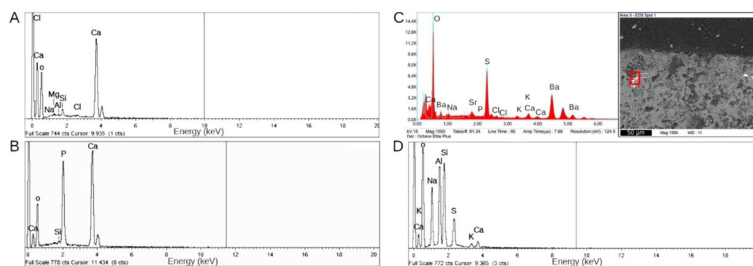
Fig. 13 EDS spectra and micro-chemical analysis of: a blue particle in Layer C (**A**); a black particle in Layer B (**B**); a barium sulphate grain impurities in Layer B (**C**) and the lime plaster from Layer A (**D**)

Moreover, SEM images have highlighted the presence of sporadic grains embedded into the greyish layer with a size of a few microns and characterized by a high radiopacity. The micro-analysis performed on these grains shows considerable concentrations of barium (70.4%) and sulphur (20.6%) pointing to the presence of barium sulphate (Fig. 13C). The SEM image shows that these barite grains are rare impurities associated with the black pictorial layer only (Fig. 13C).

The EDS spectra collected on the bluish thin pictorial film (Layer C) evidenced discrete amounts of calcium, silicon, sulphur, aluminium along with small quantities of magnesium, chlorine, sodium, and potassium, corroborating the use of ultramarine blue, previously supposed by FORS investigations. Further confirmation is given by the elemental spot analyses, punctually conducted on a blue particle, which highlighted, once again, peaks of silicon, aluminium, sodium, and sulphur univocally determining the presence of lapis lazuli (Fig. 13D).

Starting from the early Middle Ages, ultramarine blue was the most precious and expensive blue pigment used in painting [15, 37, 38]. It is obtained by the grinding of lapis lazuli, a stone mainly constituted of the mineral lazurite $(Na,Ca)_8(AlSiO_4)_6(SO_4, S, Cl)_2$ associated with calcite $(CaCO_3)$, pyrite (FeS_2) and other silicates such as diopside $(CaMgSi_2O_6)$, forsterite (Mg_2SiO_4), wollastonite $(CaSiO_3)$.

Despite the use of lapis lazuli as an ornamental stone was attested in Sumerian and Egyptian period, it was only from the sixth-seventh century that it began to be used as a pigment. The technology production of the pigment has its root in Asia, from where it was then exported to the West. Ultramarine blue was as a matter of fact detected for the first time in the wall paintings in the cave temple

at Bamiyan in Afghanistan, near the principal lapis lazuli quarries of Bamiyan. The characteristic coloration arises from the sulphur radicals inside the lazurite crystalline structure: while the S_2^- radical is a yellow chromophore, the S_3^- radical is responsible for the blue hue. [38–42].

The existence of such precious pigment in the wall paintings of the Church of the Four Holy Doctors reveals the richness of its clients. The data is even more interesting if we consider that the ultramarine blue layer was applied on a black layer.

The formula of superimposing a blue layer upon a black one became, indeed, quite popular in the post-iconoclastic period [43]. This technical expedient, especially dedicated to the execution of the backgrounds, not only makes it possible to use lower amounts of the costly pigment but at the same time, allows to improve the optical properties of the superficial blue layer by lowering the light diffusion by any white substrate, thereby achieving the desired final chromatic result and avoiding the alteration due to an excessive grinding of this blue pigment.

It is useful to underline that, as for azurite, the fine grinding of lapis lazuli is highly discouraged because of its tendency to turn towards greyish shades. However, using large-size grains means decreasing the covering power, and, in the presence of a white lime plaster, the blue colors appear attenuated. The Byzantine technique represents, in this panorama, an ingenious solution to the above-mentioned issues. From cross-section OM visible images, the thin blue layer, now gaping and thinned, does not show a regularity in the degree of grinding. Alternating larger grains of variable size on a matrix of fine grains, the artists who worked on this cycle of frescoes guaranteed the optical properties of the pigment, the

correct covering power level, also improved by the not light diffusing black background. These artistic choices have made possible to avoid a complete chromatic alteration due to overly fine grinding of blue grains, confirming a conscious use and great technological knowledge of this pigment by the unknown workshop who worked at San Marco d'Alunzio.

From the comparison with the literature, the application of a thin layer of ultramarine blue on a black layer was found in other contemporary Byzantine paintings in Southern Italy and especially in the Sardinian territory [44]. Its use is in fact attested in the mural paintings in the church of San Pietro in Galtellì (twelfth-thirteenth century, Nuoro) and those of the church of S. Nicola di Trullas in Semestene (twelfth century, Sassari). Even if the presence of blue chromophores was not evidenced in the Basilica of the Holy Trinity of Saccargia wall paintings (twelfth century, Sassari) and in the Calabrian *Déesis* of Motta San Giovanni (eleventh century, Reggio Calabria) it is reasonable to assume that a blue pictorial layer was applied above the preserved black carbon layer for the execution of the dark background, following the same procedure [45]. In the mural painting in the church of Nostra Signora di Sos Regnos Altos in Bosa (fourteenth century, Nuoro), lapis lazuli was instead mixed with black carbon pigment, revealing a variation of the original formula, also reported in literature [31].

Starting from the data obtained in situ (p-XRF and FORS analysis) and from the analytical insights achieved through laboratory equipment on sample SM4 (SEM–EDS), the XRF results on micro-fragments bearing traces of blue and black pigments (SM1 and SM3b) (Fig. 14A–E), collected from the central apse,
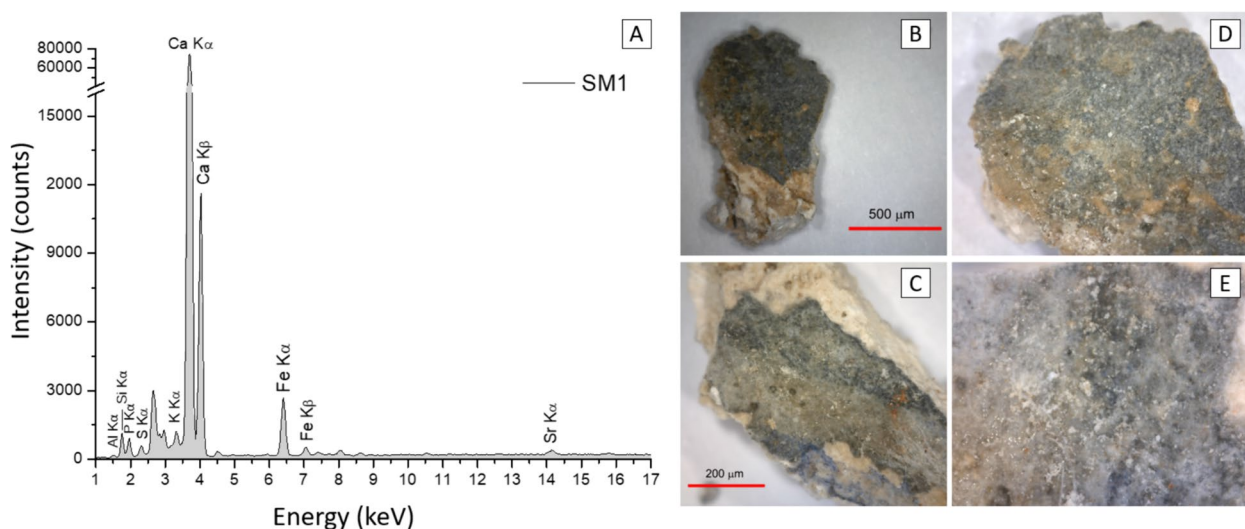
Fig. 14 XRF spectrum of the bluish pictorial layer visible in sample SM1 (**A**). Micro-graphs of sample SM1 (**B**) (**D**) and sample SM3b (**C**, **E**)

allow, by comparison, to deduce that natural ultramarine blue (of which rare granules are still visible on the surface) was also used in this area of the pictorial cycle just after the application of a bone black layer.

Furthermore, the potential use of organic binders was evaluated by the observation of sample SM4 under DOM. However, both the blue and black pictorial layers do not exhibit any diagnostic fluorescence when irradiated by UV light. Moreover, SEM–EDS analyses, punctually performed on both the pictorial layers exhibit very high concentrations of calcium, therefore suggesting the use of lime to fix the pigments on the surface. The presence of Ca signals, detected by XRF spectroscopy on all the colored areas, is coherent with the latter statement.

In addition, the micro-stratigraphical observations by SEM images and DOM examination reveal signs of a distinct separation between the blackish pictorial layer and the underlying plaster. In this regard, it is quite probable that pigments were firstly dispersed in lime and then applied on the already dried and almost carbonated plaster (i.e. *a secco* wall painting technique). Under polarized optical microscopy, the interface between the pictorial film and the plaster is clearly recognizable in the stratigraphic samples SM2 and SM5 as well, corroborating SEM and DOM analyses.

Morphological description and minero-petrographic characterization of plasters

For the characterization of the plasters and the comparison of the executive technique employed in the two apsidal wall paintings, observations were conducted with a DOM and a POM on sample SM2 (taken from the central apse) (Fig. 15A, B) and sample SM5 (collected from the right apse) (Fig. 16A).

Under reflected light, the samples show a similar stratigraphy, essentially composed of three layers with different thicknesses and textural characteristics (Fig. 15C, Fig. 16A). Starting from the support, in both the samples a first pinkish layer characterized by a coarse grain size aggregate (<1 mm). This layer, defined *arriccio*, has the function of levelling the roughness and/or the irregularities of the substrate. On this level, a further layer of white plaster was applied, mainly consisting of lime-based binder in which only rare lithic fragments or monomineralic grains can be observed (falling in the class of very fine sand i.e. 0.0625 – 0.125 mm). This layer, properly levelled, hosts a thin pictorial film.

The investigation conducted by means of POM, confirmed the previously described stratigraphic sequence. In more detail, in sample SM2 (Fig. 15D) the *arriccio* layer (thickness > 0.5 mm) shows a sandy aggregate characterized by a grain size ranging from medium-fine sand (0.125–0.2 mm) up to coarse sand (0.5 mm) with a heterogeneous distribution. It appears also very poorly sorted
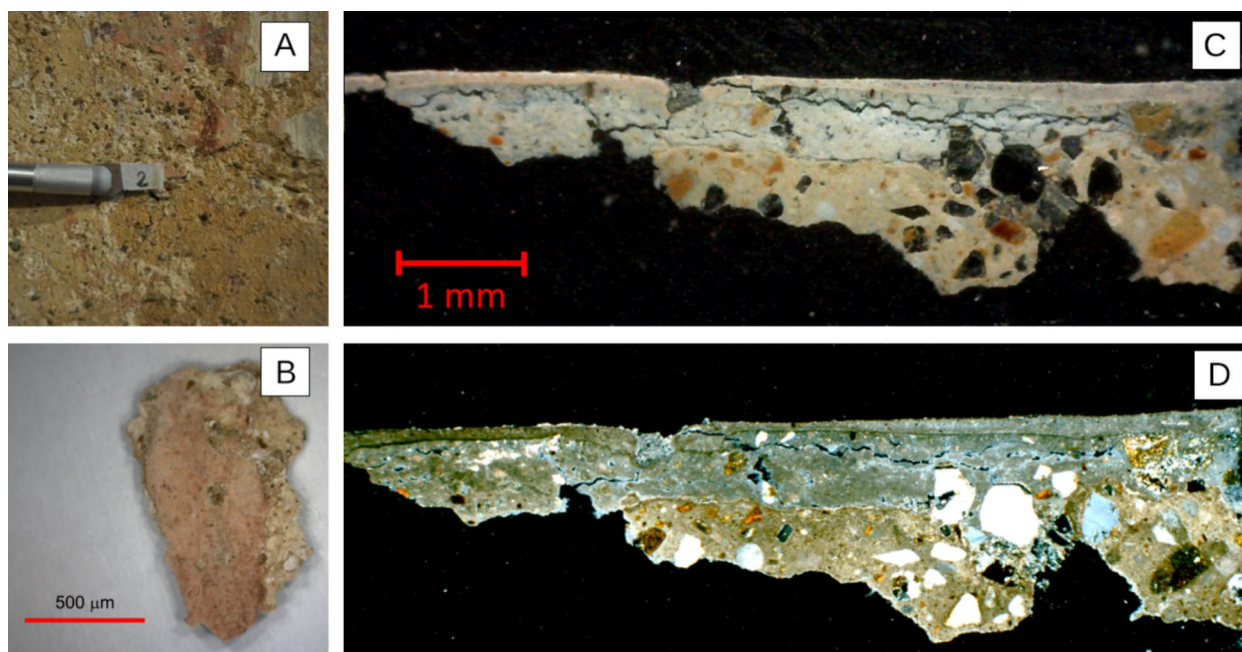
Fig. 15 Thin section micrograph under polarized light microscope of sample SM2 (crossed-nicols) (**A**) and comparison with optical microscope image in reflected light (**B**). Macroscopic image of the sampling location (**C**) and micro-graph of sample SM2 under DOM (**D**)

Alberghina *et al. Heritage Science*   (2024) 12:184

Page 15 of 17
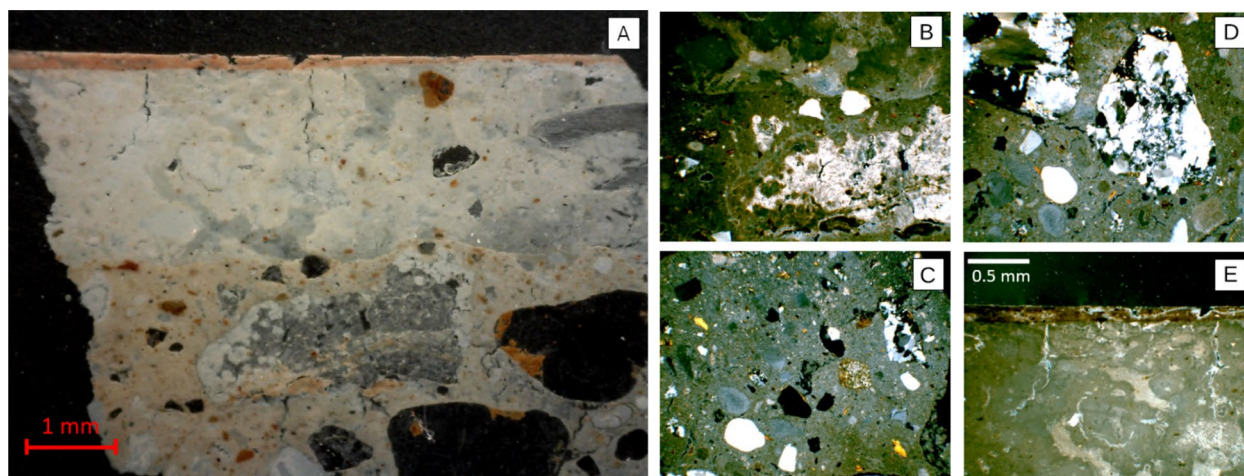
Fig. 16 Micro-photography under DOM in reflected light of sample SM5 (**A**); thin section images of the different layers (crossed polarized light) of sample SM5: upper and medium layer (**B**); medium and lower layer (**C**); lower layer (**D**); pictorial layer (**E**)

and displays angular to sub-rounded grains with medium sphericity. For what concerns the mineralogical composition, it mainly consisted of monocrystalline and polycrystalline quartz. The aggregate/binder ratio, established using standard comparison charts, varies from 4:1 to 3:1 [46]. Furthermore, the binder shows a high porosity, a heterogeneous structure, characterized by the presence of sporadic lumps of lime and a cryptocrystalline aspect. The binder matrix of the second layer is similarly characterized by a cryptocrystalline texture in which numerous shrinkage cracks running parallel to the surface are detected. Finally, the upper layer shows a thickness of 0.1 mm and it is constituted of both pigment and lime binder.

As for sample SM2, the minero-petrographic investigations carried out on sample SM5 evidenced the presence of three different layers, confirming a similar stratigraphic distribution.

The aggregate constituting the *arriccio* once again exhibits a granulometry which goes from medium-fine sand (0.125–0.2 mm) up to coarse and very coarse sand (0.5–2 mm) (Fig. 16B–D). Grains display a bimodal distribution with fragments of smaller dimensions together with larger ones. The aggregate is mainly composed of monocrystalline quartz, with a predominant size ranging between 0.5 and 0.75 mm and a common dimension of 0.125–0.25 mm, and polycrystalline ones, which reach the size of 1.5 mm. A rounded lithic fragment of carbonate nature is observed as well. Overall, the aggregate shows a roundness ranging from sub-rounded to rounded and a moderate sphericity. As for sample SM5, the binder has a moderate porosity and an isotropic aspect. Several lumps are indeed detected within the matrix. The aggregate/binder ratio

attested is about 2:1. The second layer has a thickness of 2.25 mm and it is almost entirely made of binder (Fig. 16E). Quite a few lumps and shrinkage cracks, perpendicular to the stratigraphy, are observed also in this case. Above it, it is possible to distinguish a pink separate layer of 0.125 mm, constituting the pictorial film (Fig. 16E).

Finally, it can be stated that the same executive technique was employed for the realization of the preparatory layers in the two apses. Altogether, the two samples in fact show the same stratigraphic sequence and minero-petrographic characteristics which differ only in the thickness of the layers and in the presence of some different aggregates. In particular, sample SM5, chopped in correspondence with the right apse, shows lithic fragments of carbonate nature (likely relicts of limestone after the process of calcination) absent in the other sample taken from the central altar. This difference may be due either to the different representativeness of sample SM2 which is much smaller than sample SM5 or to the random supply of raw materials, constituting the aggregate phase, in a different timing of preparation of the mortar mixtures.

The morphological and compositional characteristics of the most superficial layers (i.e., pictorial layers and lime plasters) of both the two samples are almost identical, confirming the executive contextuality of the paintings in the two apses. Finally, as previously mentioned, considering the solution of continuity at the interface between the two upper layers and the morphology of the shrinkage cracks in both cases, the pigments may have been applied on the already partially carbonated plaster, dispersing and fixing them with lime.

Alberghina *et al. Heritage Science*   (2024) 12:184

Page 16 of 17

Conclusions

The combination of the results of non-invasive investigations together with the laboratory analyses on micro-samples allowed to fully characterize the chromophores and deepen the knowledge of the executive technology of the Byzantine wall paintings preserved in the two apses belonging to the Church of the Four Holy Doctors, annexed to the Museum of Byzantine and Norman Culture and Figurative Arts of San Marco d'Alunzio (ME).

The pictorial palette is mainly characterized by ochre, red and yellow, green and brown earths. The white used as a pigment is made up of calcium carbonate, either in the form of *bianco San Giovanni* or in that of lime white. The black pigment, not identifiable by XRF or FORS due to the intrinsic limits of the two techniques, was subsequently identified by SEM–EDS, as bone black, obtained by calcination from bones.

Instrumental limits of the in situ analytical methodologies were also found in the identification of the very thin blue pictorial film superimposed on the black pictorial layer in the background area. However, the first analytical evidence, collected by means of non-invasive methodologies, suggested the possible use of ultramarine blue, as verified thanks to the results of the SEM–EDS analyses. The formula of applying a layer of ultramarine blue just after a layer of bone black was most likely also used in the central apse wall painting as proved by the XRF and optical microscopy analyses, thus confirming the contextual execution of the two adjacent pictorial evidence. The latter evidence is furthermore corroborated by the DOM and POM observations carried out on two samples taken from the central and the right mural paintings. The stratigraphy is indeed essentially composed of three layers with different thicknesses and textural characteristics. Starting from the support, the samples are constituted of an *arriccio* layer, characterized by a coarse-grained aggregate, a lime layer, and a thin layer of pictorial film. The similar stratigraphy and minero-petrographic characteristics of the plaster layers reveal the employment of the same executive technique for the realization of the two mural paintings' preparatory layers.

Abbreviations

p-XRF	Portable X-ray fluorescence
FORS	Fiber optics reflectance spectroscopy
DOM	Digital optical microscope
POM	Polarizing optical microscope
SEM	Scanning electron microscopy
EDS	Energy dispersive X-ray spectrometry
UV	Ultraviolet
SNR	Signal to noise ratio

Author contributions
MFLR, MFA, MR, SS, and LR oversaw the conceptualization of the research and methodology. MFA, SS, and LR performed formal analysis and investigation. MFA, SS, MR, and LR supervised data curation. MAZ, MFA, MR, and LR undertook the original draft preparation. MFA, MR, and LR oversaw the review and editing process. MFLR, ML, and DR made the final visualization and supervision of all the work. All authors read and approved the final manuscript.

Availability of data and materials
All data generated or analysed during this study are included in this published article.

Declarations

Competing interests
The authors declare that they have no competing interests.

References

1. Ryolo D. San Marco d'Alunzio: cenni storici e documenti. Sant'Agata Militello: Rotary Club Ed; 1980.
2. Guida MK, Rigaglia D. Gli affreschi della chiesa dei Quattro Santi Dottori a San Marco d'Alunzio: cultura artistica e restauro. Messina: Di Nicolò edizioni; 2021.
3. Kislinger E. Monumenti e testimonianza greco-bizantine di san Marco d'Alunzio (ME). Sant' Agata Militello: Rotary Club; 1995.
4. Pettignano A. Museo della cultura e delle arti figurative bizantine e normanne di San Marco d'Alunzio. Paleokastro. 2003;11:23–4.
5. De Giorgi M. La decorazione pittorica: stato di conservazione e descrizione analitica del programma pittorico. In: Brodbeck S, De Giorgi M, Jolivet-Lévy C, editors. San filippo di fragalà monastero greco della sicilia normanna, storia, architettura e decorazione pittorica. Bari: Mario Adda Editore; 2018.
6. Campagna Cicala F. Pittura medievale in Sicilia. Messina: Edizioni Magika; 2020.
7. Seccaroni C, Moioli P. Fluorescenza X—Prontuario per analisi XRF portatile applicata a superfici policrome. Firenze: Nardini editore; 2002.
8. Potts PJ, West M. Portable X-ray fluorescence spectrometry capabilities for in situ analysis. Cambridge: The Royal Society of Chemistry; 2008.
9. Bikiaris D, Daniilia S, Sotiropoulou S, Katsimbiri O, Pavlidou E, Moutsatsou AP, Chryssoulakis Y. Ochre-differentiation through micro-Raman and micro-FTIR spectroscopies: application on wall paintings at Meteora and Mount Athos. Greece Spectrochim Acta A. 2000;56:3–18.
10. Alberghina MF, Germinario C, Bartolozzi G, Bracci S, Grifa C, Izzo F, La Russa MF, Magrini D, Massa E, Mercurio M. Non-invasive characterization of the pigment's palette used on the painted tomb slabs at Paestum archaeological site. IOP Conf Ser: Mater Sci Eng. 2020;949:012002.
11. Cerrato EJ, Cosano D, Esquivel D, Jimenez-Sanchidrian C, Ruiz JR. Spectroscopic analysis of pigments in a wall painting from a high Roman Empire building in Córdoba (Spain) and identification of the application technique. Microchem J. 2021;168:106444.
12. Montana G, Giarrusso R, D'Amico R, Di Natale B, Vizzini MA, Ilardi V, Mulone A, Randazzo L, Ventura Bordenca C. Multi-analytical study of the medieval wall paintings from the rupestrian church Grotta del Crocifisso at Lentini (eastern Sicily): new evidence of the use of woad (*Isatis tinctoria*). Archaeol Anthropol Sci. 2022;14:183. https://doi.org/10.1007/s12520-022-01656-6.

13. Hradil D, Grygar T, Hradilová J, Bezdička P. Clay and iron oxide pigments in the history of painting. Appl Clay Sci. 2003;22:223–36.

14. Hradil D, Hradilová J, Bezdička P. Clay minerals in European painting of the mediaeval and baroque periods. Minerals. 2020;10:255.

15. Murat Z. Wall paintings through the ages. The medieval period (Italy, twelfth to fifteenth century). Archaeol Anthropol Sci. 2021;13:191.

16. Elias M, Chartier C, Prévot G, Garay H, Vignaud C. The colour of ochres explained by their composition. Mater Sci Eng B Solid-State Mater Adv Technol. 2006;127(1):70–80.

17. Bellanca A, Censi P, Neri R. Studio isotopico, chimico e tessiturale su materiali carbonatici associati a mineralizzazioni di fluorite e barite nell'area di Termini Imerese (Sicilia). Rend Soc Ital Mineral Petrol. 1983;38:1251–61.

18. Speciale F. Le mineralizzazioni di fluorite e barite nel territorio di termini imerese e caccamo—sicilia aspetti geologici esteriori legati alla minerogenesi. Bargheria: Eugenio Maria Falcone Ed; 2013.

19. Bacci M, Baldini F, Carlà R, Linari R. A color analysis of the brancacci chapel frescoes. Appl Spectrosc. 1991;45(1):26–31.

20. Appolonia L, Vaudan D, Chatel V, Aceto M, Mirti P. Combined use of FORS, XRF and Raman spectroscopy in the study of mural paintings in the aosta valley (Italy). Anal Bioanal Chem. 2009;395:2005–13.

21. Cheilakou E, Kartsonaki M, Koui M, Callet P. A nondestructive study of the identification of pigments on monuments by colorimetry. Int J Microstruct Mat Prop. 2009;4:112–27.

22. Cheilakou E, Troullinos M, Koui M. Identification of pigments on byzantine wall paintings from Crete (14th century AD) using non-invasive fiber optics diffuse reflectance spectroscopy (FORS). J Archaeol Sci. 2014;41:541–55.

23. Mastrotheodoros GP, Beltsios KG. Pigments—iron-based red, yellow, and brown ochres. Archaeol Anthropol Sci. 2022;14:35.

24. Zicarelli MA, La Russa MF, Alberghina MF, Schiavone S, Greca R, Pogliani P, Ricca M, Ruffolo SA. A multianalytical investigation to preserve wall paintings: a case study in a hypogeum environment. Mater. 2023;16(4):1380.

25. Ricca M, Alberghina MF, Houreh ND, Koca AS, Schiavone S, La Russa MF, Randazzo L, Ruffolo SA. Preliminary study of the mural paintings of Sotterra church in Paola (Cosenza, Italy). Mater. 2022;15:3411.

26. Hradil D, Grygar T, Hrušková M, Bezdička P, Lang K, Schneeweiss O, Chvátal M. Green earth pigment from the Kadaň region, Czech republic: use of rare Fe-rich smectite. Clays Clay Miner. 2004;52(6):767–78.

27. Moretto LM, Orsega EF, Massocchin GA. Spectroscopic methods for the analysis of celadonite and glauconite in Roman green wall paintings. J Cult Herit. 2011;12(4):384–91.

28. Cosentino A. FORS spectral database of historical pigments in different binders. E-Conser J. 2014;2:54–65.

29. Hofmann C, Rabitsch S, Malissa A, Aceto M, Uhlir K, Griesser M, et al. The miniatures of the Vienna Genesis: colour identification and painters' palettes. In: Hofmann C, editor., et al., The Vienna genesis. Wien: Böhlau Verlag; 2020. p. 201–46.

30. Aceto M, Agostino A, Fenoglio G, Idone A, Gulmini M, Picollo M, Ricciardi P, Delaney JK. Characterisation of colourants on illuminated manuscripts by portable fibre optic UV-visible-NIR reflectance spectrophotometry. Anal Methods. 2014;6(5):1488–500.

31. Gettens RJ, Stout GL. A monument of Byzantine wall painting—the method of construction. Stud Conserv. 1958;3(3):107–19.

32. Roy A, editor. Artists' pigments: a handbook of their history and characteristics. Washington: National Gallery of Art; 1993.

33. Galli A, Bonizzoni L. True versus forged in the cultural heritage materials: the role of PXRF analysis. X-Ray Spectrom. 2014;43(1):22–8.

34. Aceto M, Agostino A, Fenoglio G, Picollo M. Non-invasive differentiation between natural and synthetic ultramarine blue pigments by means of 250–900 nm FORS analysis. Anal Methods. 2013;5:4184–9.

35. Winter J. The characterization of pigments based on carbon. Stud Conserv. 1983;28(2):49–66.

36. Mayer R. The artist's handbook of materials and techniques. 3rd ed. New York, US: Viking Press; 1970.

37. Plesters J. Ultramarine blue, natural and artificial. Stud Conserv. 1966;11(2):62–91.

38. Gaetani MC, Santamaria U, Seccaroni C. The use of Egyptian blue and lapis lazuli in the Middle ages: the wall paintings of the San Saba church in Rome. Stud Conserv. 2004;49:13–23.

39. Zorba T, Pavlidou E, Stanojlovic M, Bikiaris D, Paraskevopoulos KM, Nikolic V, Nikolic PM. Technique and palette of XIIIth century painting in the monastery of Mileseva. Appl Phys A. 2006;83:719–25.

40. Osticioli I, Mendes NF, Nevin A, Gil FP, Becucci M, Castellucci E. Analysis of natural and artificial ultramarine blue pigments using laser induced breakdown and pulsed Raman spectroscopy, statistical analysis and light microscopy. Spectrochim Acta Part A Mol Biomol Spectrosc. 2009;73(3):525–31.

41. De Benedetto GE, Fico D, Margapoti E, Pennetta A, Cassiano A, Minerva B. The study of the mural painting in the 12th century monastery of Santa Maria delle Cerrate (Puglia-Italy): characterization of materials and techniques used. J Raman Spectrosc. 2013;44(6):899–904.

42. Farsang S, Caracas R, Adachi TB, Schnyder C, Zajacz Z. S_2^- and S_3^- radicals and the S_4^{2-} polysulfide ion in lazurite, haüyne, and synthetic ultramarine blue revealed by resonance Raman spectroscopy. Am Mineral. 2023;108(12):2234–43.

43. Mora P, Mora L, Phipilippot P. La conservazione delle pitture murali. Bologna: Compositori; 1999.

44. Solla L. Segni e colori nel telaio del tempo: tracce, luce e materia nella policromia della Sardegna. Contributo alla conoscenza e conservazione di dipinti murali romani e medievali. PhD Thesis. Cagliari: University of Cagliari; 2016. Available from: https://core.ac.uk/download/pdf/35316414.pdf.

45. Salatino G, Zicarelli MA, Ricca M, Macchia A, Randazzo L, Pogliani P, Arcudi A, Ruffolo SA, La Russa MF. A multi-analytical diagnostic on an outdoor wall painting: the study on the Déesis of St. Maria Annunziata's church, Motta San Giovanni (Reggio Calabria, Italy). Appl Sci. 2023;13(18):10439.

46. Matthew AJ, Woods AJ, Oliver C. Spots before your eyes: new comparison charts for visual percentage estimation in archaeological material. In: Middleton A, Freestone I, editors. Recent developments in ceramic petrology, (British Museum Occasional Paper 81). London: The British Museum; 1991.

Publisher's Note